JPP JOURNAL OF Pharmacy and Pharmacology
ROYAL PHARMACEUTICAL SOCIETY
JPP Journal of Pharmacy And Pharmacology
Research Paper

Protein-coated nanoparticles embedded in films as delivery platforms

Javier O. Morales[a,c], Alistair C. Ross[d] and Jason T. McConville[b]

[a]College of Pharmacy, The University of Texas at Austin, Austin, TX, [b]University of New Mexico, Albuquerque, NM, USA, [c]School of Chemical and Pharmaceutical Sciences, University of Chile, Santiago, Chile and [d]Ferring Controlled Therapeutics Ltd, East Kilbride, Scotland, UK

Keywords
antisolvent precipitation; buccal delivery; enzyme activity; films; protein-coated nanoparticles

Correspondence
Jason T. McConville, 2705 Frontier NE, Albuquerque, NM 87131, USA.
E-mail: jmcconville@unm.edu

Received November 16, 2012
Accepted January 29, 2013

doi: 10.1111/jphp.12046

Abstract

Objectives This work aimed to evaluate the performance of nanoparticle-loaded films based on matrices of polymethacrylates and hydroxypropylmethylcellulose (HPMC) intended for delivery of macromolecules.

Methods Lysozyme (Lys)-loaded nanoparticles were manufactured by antisolvent co-precipitation. After size, loading efficiency and stability characterization, the selected batch of particles was further formulated into films. Films were characterized for mechanical properties, mucoadhesion, Lys release and activity after manufacture.

Key findings We found that protein-coated nanoparticles could be obtained in USP phosphate buffer pH 6.8. Particles obtained at pH 6.8 had a z-average of 347.2 nm, a zeta-potential of 21.9 mV and 99.2% remaining activity after manufacture. This formulation was further studied for its application in films for buccal delivery. Films loaded with nanoparticles that contained Eudragit RLPO (ERL) exhibited excellent mechanical and mucoadhesive properties. Due to its higher water-swelling and solubility compared with ERL, the use of HPMC allowed us to tailor the release of Lys from films. The formulation composed of equal amounts of ERL and HPMC revealed a sustained release over 4 h, with Lys remaining fully active at the end of the study.

Conclusions Mucoadhesive films containing protein-coated nanoparticles are promising carriers for the buccal delivery of proteins and peptides in a stable form.

Introduction

The recent increase in the number of products under review by the US Food and Drug Administration (FDA) or undergoing late-phase clinical trials demonstrates that protein and peptide therapeutics is a rapidly growing field in the pharmaceutical industry.[1] However, it is widely reported in the literature that the efficacious delivery of these therapeutic agents is the determinant factor in product development.[2,3] Therefore, to achieve the real potential of protein and peptide therapeutics, effective smart delivery platforms and strategies to overcome the formulation and delivery challenges need to be developed. The conventional approach for the delivery of macromolecules is through injections.[4] This method of delivery is largely associated with drawbacks in patient compliance and acceptance; the start of therapy can be delayed and patients can develop needle anxiety.[5] In addition, the number of injections may lead to compliance issues[6] in therapies that rely on this route of administration. Therefore, alternative routes of delivery are vital to achieve a broad platform of successful product development.

Among alternative routes of delivery for proteins and peptides, the oral route has long been widely investigated.[7,8] However, several drawbacks associated with the gastrointestinal tract make the development of novel delivery platforms for macromolecules very challenging. Instability in gastric pH, proteolytic enzyme content in the upper gastrointestinal tract and insufficient permeation and bioavailability has limited the success that has been achieved.[9] These

limitations have led to the exploration of other routes of delivery, such as pulmonary, nasal and transdermal routes. Particularly, the buccal route of delivery offers interesting advantages in comparison with the oral route and its associated gastrointestinal-tract limitations for the delivery of protein and peptides.[9] In bypassing absorption via the gut, the stability of macromolecules may not be compromised before reaching the circulation. Other advantages of this route of delivery, such as its good vascular drainage, ease of administration and relatively low enzyme levels, make it a good candidate for the delivery of proteins and peptides.[10]

Mucoadhesive films as dosage forms for the buccal route of delivery have been investigated in the past decade but little effort has been made with regards to the delivery of proteins and peptides as particulate forms.[11,12] From a formulation standpoint, actives are usually added to the film by their inclusion in the casting solution, then allowing the solution to dry into the solid form. However, in general the polymers used in formulations containing proteins are more hydrophobic in comparison with the hydrophilic nature of proteins.[8] This could potentially lead to precipitation of proteins during storage, or *in vivo*, leading to possible instability.[13] Additionally, strategies such as incorporating insulin as a solid solution into poly(lactic-*co*-glycolic acid) (PLGA) microspheres, to prevent chemical reactions in the solid state and to control the peptide release, have been unsuccessful. During PLGA erosion, the microenvironmetal pH drops and deamidation has been found to be the main reaction that causes insulin instability.[14] For the delivery of insulin, chitosan seems to be a more suitable candidate as a polymer vehicle. Cui *et al*. have developed chitosan–ethylenediaminetetracetic acid (chitosan–EDTA) films containing insulin for buccal delivery and have demonstrated the retention of the physical structure of the peptide upon release.[15] However, there is no mention of the uniformity of the drug in the film upon solidification and this prohibits any conclusion about drug distribution homogeneity. More recently, Giovino *et al*. have developed chitosan films for the buccal sustained delivery of insulin in polyethylene glycol-*b*-polylactic acid (PEG-*b*-PLA) nanoparticles as a model for buccal macromolecular delivery.[16] Although adequate physico-mechanical properties were achieved, very high heterogeneity was revealed by the mechanical variables studied (time to break, tensile strength, Young's modulus and work done to break). This therefore raises concern over the tight control of manufacture necessary to prepare films with homogeneous particle distribution, adequate physico-mechanical properties, high loading efficiency and retention of macromolecule activity.

In recent years, investigations of enzyme immobilization in organic solvents have opened the door for the manufacture of particulate-containing films with enhanced activity. Especially, the antisolvent co-precipitation method has been shown to produce particles coated with a variety of biologicals including nucleic acids, proteins, enzymes and other particulate systems.[17,18] However, most of these investigations led to particles in the range of 1–5 μm or higher. To guarantee physical stability of the films in terms of both mechanical and mucoadhesive properties, such large particles are undesirable due to the potential for aggregation and loss in active distribution homogeneity.[19] Our group has recently described the manufacture of submicron and nanosized particles of lysozyme (Lys)-loaded D,L-valine (Val), also known as protein-coated nanoparticles (PCNPs), and the advantages of this method of manufacture to provide high loading efficiency and enzymatic stability.[20] Based on our previous investigations, it is known that a combination of high mixing energy provided by a probe sonicator, the addition of the aqueous phase by means of a nebulizer and the use of surfactant as a stabilizer can altogether yield relatively narrowly distributed PCNPs. Here, we sought to study the performance of PCNP-containing films based on polymer matrices of polymethacrylates and hydroxypropylmethylcellulose (HPMC) that are ultimately intended for buccal delivery of macromolecules.

Materials and Methods

Materials

Val and Lys were obtained from Sigma-Aldrich (St Louis, MO, USA). Sorbitan monostearate (Span 60) was obtained from Spectrum Chemical (New Brunswick, NJ, USA). Eudragit RSPO and RLPO (ERS and ERL) were kindly donated by Evonik Industries (Darmstadt, Germany). Carbopol 974P (C974P) and Noveon AA-1 Polycarbophil (PCP) were donated by Lubrizol Advanced Materials (Cleveland, OH, USA). HPMC (Methocel E50 Premium LV) was donated by Colorcon (Harleysville, PA, USA). Triethylcitrate (TEC; Vertellus Specialties Inc., Indianapolis, IN, USA), mucin (Spectrum Chemical) and *Micrococcus lysodeikticus* (Worthington Biochemical Corp., Lakewood, NJ, USA) were purchased and used as received. HPLC-grade isopropanol (IPA) was obtained from Fisher Scientific (Fair Lawn, NJ, USA) and de-ionized water was procured in house (Milli-Q Direct; Millipore, Billerica, MA, USA). All other chemicals used were of analytical or reagent grade.

Protein-coated nanoparticle manufacture

The manufacturing process for PCNPs was based on antisolvent co-precipitation and our approach has been recently published elsewhere.[20] Briefly, the co-precipitant Val and the amount of Lys to be precipitated were dissolved in one of the buffers (all with a concentration of 50 mM) and solutions studied to observe the effect of pH on the manufacturing process (Table 1). First, Val was dissolved in the

Table 1 Formulations prepared to study the effect of pH in the manufacturing process of Lys PCNPs

Formulation	Protein model	Buffer/solution	pH
SPH01	Lys	N Phthalate	5.4
SPH02	Lys	Phosphate	6.8
SPH03	Lys	Borate	10
SPH04	Lys	NaOH	13

aqueous phase at a concentration of 61.2 mg/ml (or 90% of its saturation concentration) and then Lys was dissolved in this solution to yield a protein content of 40% w/w based on solid content. By means of an Aeroneb Pro vibrating mesh nebulizer (Aerogen, Galway, Ireland), the aqueous phase was then added to the antisolvent organic phase. The organic solvent must be miscible with water to promote the fast dehydration of the precipitant and co-precipitant. We have shown previously that IPA containing Span60 was the most effective antisolvent yielding smaller particle sizes;[20] therefore, a 0.008 mM Span 60 solution was used. Finally, during the addition of the aqueous phase, high-energy mixing was provided by means of a Branson Sonifier 450 probe sonicator (Branson Ultrasonics, Danbury, CT, USA). After addition of the total volume of aqueous phase, sonication was maintained for 20 more minutes to further stop particle growth during the early stages of coagulation.[20]

Particle sizing

To determine the particle size of the slurries obtained in IPA a Zetasizer Nano ZS (Malvern Intruments Ltd, Malvern, UK) was used. Using the Mie theory and a scattering angle of 173°, mean particle size was obtained as a z-average, which corresponded to the intensity weighted mean hydrodynamic size measured by dynamic light scattering (DLS). Additionally, an estimate of the width of the distribution was obtained from the instrument as a polydispersity index (PdI). Approximately 1 ml of IPA slurry directly obtained from the manufacturing process was analysed by DLS in disposable polystyrene cuvettes (1 cm path length). A total of three to five 5 determinations of 15–20 runs each were conducted. For these determinations, the real and imaginary refractive indices used were 1.590 and 0.010, respectively.

Zeta-potential determination

Zeta-potentials (ZP) of slurries were obtained by laser Doppler micro-electrophoresis using a Malvern Zetasizer Nano ZS (Malvern Instruments Ltd). Approximately 1 ml of slurry directly obtained from the manufacturing process was added to a polycarbonate capillary cell for determination of zeta-potential. A total of five determinations of 14–20 runs each were conducted at 150 V to obtain the average zeta-potential of the slurries.

Lysozyme quantification by reverse-phase high-performance liquid chromatography

Chromatography was performed using a Zorbax 300SB C18 Rapid Resolution column (3.5 μm, 4.6 mm inner diameter × 150 mm length; Agilent Technologies, Santa Clara, CA, USA).The mobile phase consisted of two solvents with different polarities: solvent A consisted of water with 5% v/v acetonitrile and 0.1% v/v trifluoroacetic acid; solvent B consisted of acetonitrile with 5% v/v water and 0.085% v/v trifluoroacetic acid. The mobile phase consisted initially of 10% v/v solvent B and was maintained for 3 min followed by a solvent gradient of 60% v/v solvent B for 16 min and then a drop back to 10% v/v maintained for 1 min, for a total run time of 20 min. The flow rate was set to 1 ml/min and temperature remained constant at 25 °C. The injection volume was 50 μl and the UV detector was set to 215 nm. Under these conditions, Lys eluted at about 11.1 min. The reverse-phase high-performance liquid chromatography (RP-HPLC) method was validated and exhibited adequate linearity, accuracy and reproducibility (relative standard deviation < 0.1%). For the determination of Lys loading efficiency, particles were separated by centrifugation at 18 000*g* (Avanti J 25; Beckman, Fullerton, CA, USA) then dried overnight at room temperature with a positive air flow. The solids were then resuspended in pH 6.8 phosphate buffer (50 mM) and Lys was quantified using the RP-HPLC method. To compute Lys loading efficiency, the percent mass ratio of Lys in the formulation to the Lys initially added to the manufacturing process was calculated. To determine the content of Lys in films, release of Lys was allowed to occur over 24 h at 37 °C in pH 6.8 phosphate buffer (50 mM) in an orbital shaker (Environ Shaker 3527; Lab-Line Instruments, Melrose Park, IL, USA) and then the media assayed by RP-HPLC.

Lysozyme activity with *Micrococcus lysodeikticus*

The enzymatic activity of Lys after manufacture of particles was determined turbidimetrically based on the Shugar method.[21] Activity was correlated with a decrease in absorbance at 450 nm of solutions containing *Micrococcus lysodeikticus* due to the lytic activity of Lys on the cell walls. A 0.3 mg/ml cell suspension (0.9 ml) was mixed with a stock lysozyme pH 6.2 phosphate buffer solution containing 0.1 mg/ml (0.1 ml) to determine the maximum lytic effect. After separation and drying of particles, the solid was dissolved in a pH 6.2 phosphate buffer (50 mM) to a concentration of 0.1 mg/ml. Following the same procedure, sample solutions were assayed against a suspension of

Table 2 Film formulation compositions and mucoadhesive controls (as % w/w) that were studied to investigate the performance of films containing SPH02

Formulation	Eudragit RL	Eudragit RS	HPMC	C974P	PCP	TEC	IPA solution
FPH01	90	–	–	–	–	10	SPH02
FPH02	73	–	17	–	–	10	SPH02
FPH03	64	–	26	–	–	10	SPH02
FPH04	45	–	45	–	–	10	SPH02
FPH05	–	90	–	–	–	10	SPH02
FPH06	90	–	–	–	–	10	Lys[a]
C974P	–	–	–	90	–	10	–
PCP	–	–	–	–	90	10	–

[a]Unprocessed Lys was dispersed in IPA to prepare the control formulation FPH06.

M. lysodeikticus and absorbance was measured at 450 nm to determine maximum activity of solutions. Relative activity was calculated considering the absorbance measured for a fresh Lys stock solution as 100% activity. To determine the remaining relative activity of Lys in films, the same media obtained after overnight shaking described in the above section on Lys quantification by RP-HPLC, was used.

Preparation of particle-containing films

Casting solutions were prepared by combining two organic solutions and cast overnight in polytetrafluoroethylene molds. Acetone was used to dissolve or suspend the polymer combinations as depicted in Table 2. This solution was combined in a solvent mixture of acetone–IPA (4 : 6) with suitable amounts of SPH02 (pH 6.8) of Lys-containing IPA (for the control formulation, FPH06) to yield the final casting solution. Control formulations were manufactured utilizing C974P and PCP as mucoadhesive models, well known for their mucoadhesive character in the literature (Table 2). After 24 hours, films were peeled off and stored in aluminium foil sachets in a dessicator until characterization.

Morphology of particles and films

A scanning electron microscope (Quanta 650 FEG; FEI Company, Hillsboro, OR, USA) was used for imaging and ultrastructure analysis of both particles and particle-containing films. After separation and drying of slurries, samples were mounted onto aluminium stubs using conductive carbon tape for coating. For the imaging of films, cross-sections were obtained by a freeze-fracture method to ensure clean-cut edges and to avoid plastic deformation (often resulting from mechanical cutting). Fragments of the surface of the film were frozen by submerging in liquid nitrogen and then cracked. Pieces of the films were fixed on aluminium stubs by means of conductive carbon tape for coating. Coating was performed, using a 208 HR Cressington sputter coater (Cressington Scientific Instruments Ltd, Watford, UK) with Pt/Pd, to a thickness of 10–15 nm in a high-vacuum evaporator. To avoid structural deformation during imaging, the electron beam voltage was kept at 2–5 kV.

Mucoadhesive and mechanical properties of films *in vitro*

Mucoadhesion tests were conducted on a TA.XTPlus texture analyser (Stable Micro Systems, Godalming, UK) equipped with a 5 kg load cell. Briefly, films were held in the horizontal position and 5 µl of model mucus (a freshly made 2% w/v mucin solution) was placed on top of the film. This amount was sufficient to mimic the average saliva thickness. A stainless-steel cylindrical probe (7 mm diameter) was attached to the mobile arm of the texture analyser and it was brought into contact with the film and mucin solution, held at an applied force of 50 mN for 15 s and then withdrawn at a rate of 0.5 mm/s. The mucoadhesive force (MAF) and work of adhesion (WoA) were obtained from the peak and the area under the curve in the force-versus-distance profile, respectively.

For the determination of mechanical properties, rectangular strips of 1×5 cm^2 were cut and 1 cm on each end was held between clamps attached to the texture analyser, leaving a testing area of 1×3 cm^2. The upper clamp (connected to the mobile arm of the texture analyser) was moved upwards at a rate of 0.5 mm/s until film failure. Stress was determined from the force measurements obtained from the instrument divided by the cross-sectional area of the film, while strain was computed by dividing the increase in length by the initial film length. From the plot, the tensile strength (TS) and the elongation at break (EB) were obtained from the peak stress and the maximum strain, respectively, also represented by the following equations:[12]

$$Tensile\ strength\ (TS) = \frac{Peak\ stress}{Cross\text{-}sectional\ area\ of\ \ film} \quad (1)$$

$$Elongation\ at\ break\ (EB) = \frac{Increase\ in\ length\ at\ break}{Initial\ film\ length} \times 100 \quad (2)$$

Additionally, the elastic modulus (EM) was obtained from the initial elastic deformation region in the stress versus strain plot.[22] Since the rate of the mobile arm extension was constant for all samples tested, direct comparison of the slope in this region can be done. To further evaluate mechanical properties three additional parameters were computed from the conventional mechanical parameters obtained from the plot as follows:[23]

$$Tensile\ strength\ to\ modulus\ ratio = \frac{TS}{EM} \quad (3)$$

$$Relative\ surface\ energy\ (RSE) = \frac{TS^2}{2 \times EM} \quad (4)$$

$$Toughness\ index\ (TI) = \frac{2}{3} \times TS \times EB \quad (5)$$

Lysozyme release and kinetics analysis

Lys release was performed using Franz diffusion cells (under occlusion) with 50 mM phosphate buffer pH 6.8 as medium. To support the films and avoid solid disintegration into the receiving chamber, a 0.1 μm nylon membrane filter was additionally placed between the donor and receptor compartment. We found that said pore size did not limit diffusion; therefore, this did not have an impact in the release properties from the films (data not shown). Films were cut into circular samples (1.5 cm diameter, $n = 3$) and allowed to release into the reservoir medium for 4 h. At intervals of 0.25, 0.5, 1, 2, 3, and 4 h, 300-μl samples were withdrawn and replaced with fresh media. The Lys content was determined using the RP-HPLC method described above.

To analyse the mechanisms involved in the release of Lys, kinetics models were compared to the release profiles. The Higuchi, Korsmeyer–Peppas and first-order kinetic models were used to fit the data and were compared on the basis of R^2 adjusted.[24] The evaluation of the drug transport mechanism was addressed in accordance with the Korsmeyer–Peppas model.

Statistical analysis

All statistical analyses were performed with the software Minitab Release 14 (Minitab Inc., State College, PA, USA). One-way analysis of variance was used for multiple comparisons and Tukey's post-hoc pairwise comparisons were performed to compare which results led to significant differences. For the evaluation of the kinetics models and calculation of adjusted R^2 values, Origin 8.0 software (Northampton, MA, USA) was used to perform non-linear regressions for each kinetic model equation. All values are reported as the mean and standard deviation of the mean (SD) is shown in parenthesis.

Results and Discussion

Effect of pH on the particle manufacturing process

We previously reported a method for the manufacture of submicron and nanosized particles containing Lys by an antisolvent co-precipitation method.[20] The optimized method of manufacture consisted of the use of a nebulizer to add the aqueous phase into the surfactant-containing organic phase under a high-energy mixing input generated by a probe sonicator. Here we investigated the effect of pH in the aqueous phase containing Lys on particle size, loading efficiency and stability, among other variables.

A narrow particle size distribution was obtained at optimized conditions. Due to a limit of solubility of Val and supersaturation in the aqueous phase upon addition of Lys, we were unable to manufacture SPH01 particles. SPH02 at pH 6.8 was found to be the best condition for the precipitation of Lys. This formulation yielded very small particle sizes (347.2 ± 16.9 nm), adequate PdI in the range of 0.2–0.4,[25,26] and low variability (Table 3). The flake-like shape of particles obtained for SPH02 were in agreement with previous findings obtained by inspection under the scanning electron microscope (Figure 1).[20] As we have

Table 3 Particle size reported as z-average, polydispersity index and zeta-potential of Lys formulations

Formulation	Z-average (nm)*	Polidispersity index*	Z-Potential (mV)
SPH01	–[a]	–[a]	–**
SPH02	347.2 (16.9)	0.36 (0.02)	21.9 (3.7)**
SPH03	1384.0 (152.7)	0.28 (0.13)	18.3 (2.0)**
SPH04	1220.2 (426.6)	0.43 (0.13)	10.1 (1.2)

Results are represented as the mean (SD). *Among parameters, all differences were statistically significant ($P < 0.05$). **Non-significant differences ($P < 0.05$). [a]Co-precipitant and Lys did not dissolve at pH 5.4.

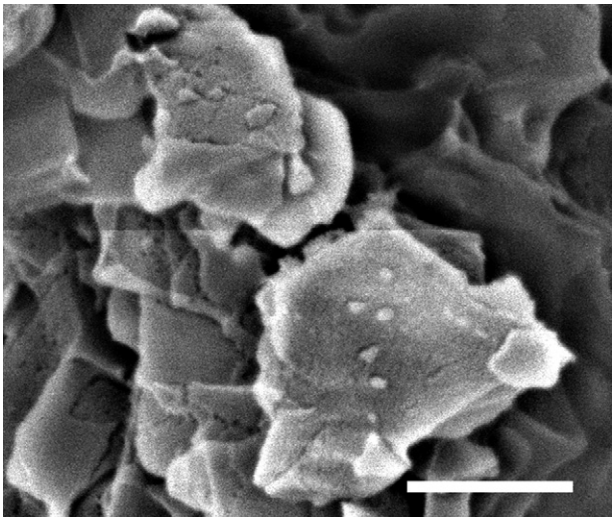

Figure 1 SEM micrograph of protein-coated nanoparticles from formulation SPH02. Scale bar =1 μm (Data are means ± SD, $n = 5$).

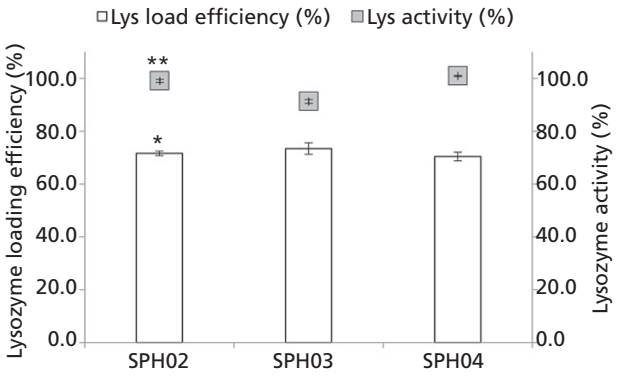

Figure 2 Lys loading efficiency (■) and relative activity (□) of Lys-containing particle formulations. $*P < 0.05$, no significant differences were found among Lys loading efficiency results. $**P < 0.05$, all the activity results were significantly different from each other (Data are means ± SD, $n = 3$).

previously shown, during the antisolvent precipitation process and due to the very high concentration of co-precipitant (i.e. Val), the particle takes on the shape of the core-forming material.[20] The active then precipitates on the surface of the growing nanoparticle and, much like a surfactant, hinders further growth by coagulation or condensation.[27] The asymmetrical shape of the flake-like particles also has an impact on the resulting particle size and PdI obtained by DLS.[28] Having very high length-to-thickness ratio, homogeneity measured by the PdI is increased. Jores *et al.* reported similar findings after manufacturing platelet-like solid lipid nanoparticles and nanostructured lipid carriers. Asymmetrical particle shape was found to increase PdI values to the range of 0.1–0.3.[28] The ZP found for SPH02 is well correlated with particles in the nano size and the magnitude indicates good dispersion stability of the formulation.[29] Even though slurries obtained here were rapidly needed in the process of manufacturing films embedded with particles (typically 5–10 min lapsed after particle manufacture and the start of the film manufacturing process), visual observations hinted at the greater dispersion stability of SPH02. During a one-week period, particles in the SPH02 slurry remained in suspension in comparison with any of the other formulations which sedimented shortly after manufacture.

Regardless of the pH, excellent Lys loading efficiency and stability was achieved. With loading efficiencies in the range of 70.5–73.4 (no statistical differences found, $P < 0.05$) and remaining relative activity in the range of 91.4–101.1%, we corroborated that the method of manufacture of nanoparticles by the antisolvent co-precipitation method is successful in rendering functional particles (Figure 2). This also indicates that the pH of the buffer solution containing Lys before manufacture had little effect on the resulting stability after manufacture. Investigations on the manufacture of microparticles in the range of 1–10 μm obtained through a similar process of antisolvent co-precipitation have shown positive results regarding the stability of the macromolecules coating an inert core.[27,30] Our findings here constitute an improvement over the particles obtained previously where the optimized conditions allowed for a z-average of 439 nm with a loading efficiency around 50% and remaining activity of 98.7%.[20] We were also able to obtain nanoparticles with a much higher enzyme load (40% instead of 10% w/w), which represents an advantage in terms of dosing in the final dosage form.

Development of lysozyme particle-containing films

Films were successfully manufactured and their surface appeared homogeneous to the eye. A close inspection revealed a smooth surface in films without HPMC, while films that contained HPMC presented with a rougher surface (resulting from the composite nature of the ERL-HPMC matrix). Regardless of the roughness observed in HPMC-containing films, the area-normalized weight was around 100 mg/cm^2 with no statistically significant difference between formulations ($P > 0.05$, Table 4). The incorporation of HPMC in ERL films resulted in a tendency to increasing thickness, being significantly different only at the highest content of HPMC. The hydrophilic character of HPMC results in swelling upon dispersion in the solvent mixture, and after drying remains in a less-dense state than ERL.[31] A similar trend for increase in thickness and surface roughness with an increase in HPMC content has been described by Ham *et al.* in films for the vaginal delivery of a

Table 4 Area-normalized weight, thickness and mechanical properties for Lys-containing films. Results are represented as the mean and standard deviation in parenthesis

Formulation	Weight* (mg/cm^2)	Thickness (μm)	Tensile strength (N/mm^2)	Elongation at break (%)	Elastic modulus (N/mm^2/%)
FPH01	98.3 (4.0)	428.7 (14.4)	1.653 (0.160)^{a}	197.9 (26.7)^{a}	0.318 (0.110)^{a,b}
FPH02	100.5 (4.2)	449.0 (18.1)	2.783 (0.133)	50.0 (11.0)^{b,c}	0.831 (0.048)
FPH03	93.0 (4.9)	433.3 (26.7)	5.169 (0.462)^{b}	25.6 (6.5)^{b,d}	1.554 (0.191)
FPH04	101.9 (8.7)	556.6 (29.4)**	5.005 (0.464)^{b}	18.0 (4.0)^{c,d}	1.228 (0.129)
FPH05	103.8 (4.7)	367.4 (16.6)**	0.580 (0.075)^{c}	233.6 (43.9)^{a}	0.153 (0.038)^{a}
FPH06	101.9 (0.5)	439.7 (13.8)	1.273 (0.124)^{a,c}	124.7 (12.9)	0.465 (0.093)^{b}

Results are represented as the mean (SD). *No significant differences were found among area-normalized weight of formulations. **Among thickness variation, only FPH03 and FPH04 are different from each other and all the rest. $^{a-d}$Among parameters, non-significant differences are indicated in pairs of letters ($P < 0.05$).

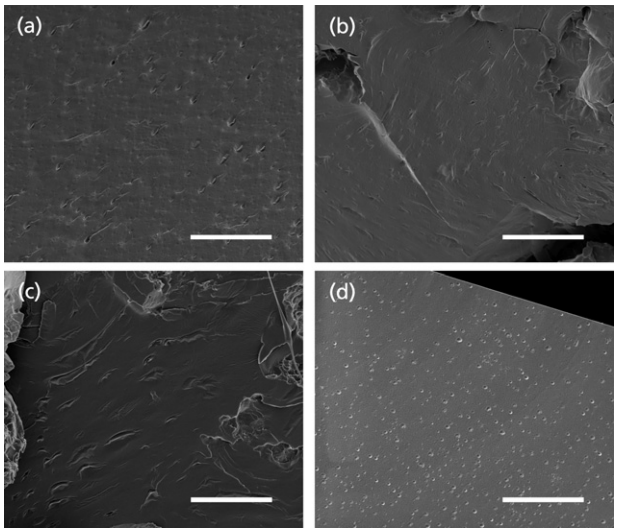

Figure 3 SEM micrographs of cross-sections of films obtained by freeze-fracture. (a) FPH01, (b) FPH03, (c) FPH04, and (d) FPH05. Scale bar represents 20 μm.

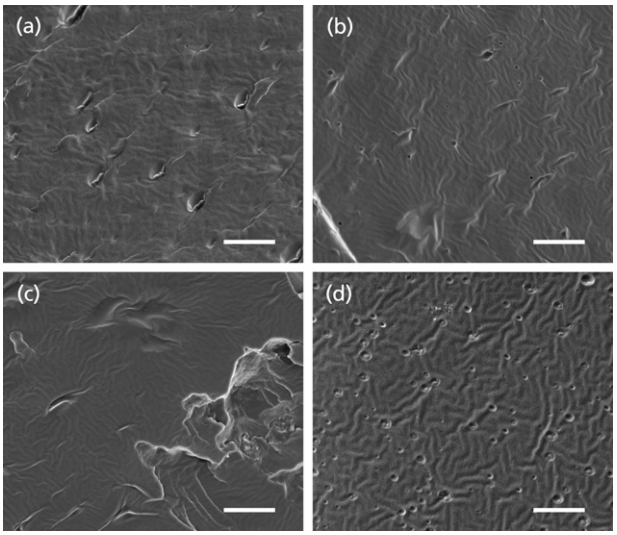

Figure 4 SEM micrographs of cross-sections of films obtained by freeze-fracture. (a) FPH01, (b) FPH03, (c) FPH04, and (d) FPH05. The bar represents 5 μm.

pyrimidinedione.[32] Scanning electron microscopy (SEM) observation of cross sections of selected film formulations obtained by freeze-fracture revealed a uniform distribution of the flake-like particles throughout the polymeric matrix (Figure 3). A closer look (Figure 4) showed that mostly individual particles were separately enclosed resulting in a high drug content uniformity in the films. As mentioned above, agglomerates of HPMC can also be observed homogeneously distributed under SEM, indicating the composite nature of the film that is responsible for the rough characteristic of the HPMC-ERL matrix.

Mucoadhesion and mechanical properties of lysozyme-containing films

ERS and ERL are more commonly known for their applications in sustained drug delivery by controlling drug release rate of dosage forms. However, more recently we have reported on the high mucoadhesive properties exhibited by polymethacrylates and, more specifically, ERL.[19] In accordance with our previous findings, films containing ERL showed high or very high mucoadhesive properties. Figure 5 shows that FPH01 had a much higher WoA than any of the other formulations studied and more than the mucoadhesive controls studied, namely C974P and PCP ($P < 0.05$). Additionally, among the series of formulations studied (FPH01–06), FPH01 exhibited a significantly higher MAF ($P < 0.05$). We believe that the presence of water-soluble particles homogeneously distributed among the film surface allows for a more rapid and homogeneous water penetration. According to the theories of mucoadhesion based on diffusion and water penetration,[33] the presence of water in the interface is paramount for the establishment of the mucoadhesive bond. The water rapidly driven in by the water-soluble molecules allows for polymer chain mobility resulting in entanglement with the mucin molecules in the

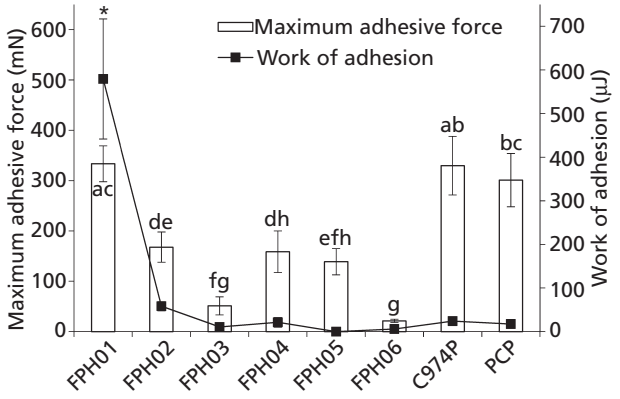

Figure 5 Mucoadhesive properties of Lys-containing films. The same values for conventional mucoadhesive polymers, such as C974P and PCP, are depicted for comparing the performance of films developed here. a–h. Non-significant differences among maximum adhesive force are indicated in pairs of letters ($P > 0.05$). *Only work of adhesion of FPH01 was significantly different from other formulations ($P < 0.05$). All other values were not statistically different ($P > 0.05$) (Data are means ± SD, $n = 5$).

mucus layer and establishment of the mucoadhesive bond. Similar effects have been found in systems wherein the drug was incorporated as particulate material. Panomsuk *et al.* have described that the inclusion of a water-soluble drug, such as theophylline, increases the amount of water associated with the polymer, favouring gelling and swelling.[34] It has also been shown that the presence of particulate material interrupts the polymer matrix continuum; this allows the polymer chains to move more freely, leading to an increase in water penetration.[35] The absence of particulate material in the formulations containing only C974P and PCP leads to their inherent mucoadhesion resulting from the capacity of the polymer to absorb water and plasticize the polymer chains to interact with mucin. It should be noted that the addition of HPMC hinders the full extent of mucoadhesion enhancement possibly by capturing the particles (that are more hydrophilic) in HPMC-rich domains. This results in slower hydration and thus a weaker mucoadhesive bond that mostly depends on the mucoadhesion of HPMC. HPMC has been used in the past as a mucoadhesive material but its mucoadhesive power is lower than that observed for PCP and C974P.[36] A similar trend was found in investigations by Wong *et al.* performed on films composed of a polymethacrylate and HPMC.[37] The authors found that an increase in the HPMC concentration resulted in a decrease in mucoadhesion. We believe that higher contents than 30% make a substantial change in the material properties and the inherent mucoadhesivity of HPMC starts to play a role at high contents. The polymer matrix of FPH04 was equally composed of HPMC and ERL (% w/w) resulting in an increase in mucoadhesion compared with FPH03 (Figure 5). At this higher HPMC content, the inherent mucoadhesion becomes more dominant in the interaction resulting in an overall higher mucoadhesion, overriding the detrimental effect of encapsulating the water-soluble particles. However, the mucoadhesive properties of FPH04 were still below those observed for FPH01. Finally, ERS exhibited higher MAF than the ERL films with drug in solid solution.[19] This is interesting considering that ERS is the more hydrophobic material due to its lower content of quaternary ammonium groups. We have previously shown that ERS consistently exhibits lower MAF and WoA than ERL.[19] However, we believe that the enhancing effect of the water-soluble particulate material discussed earlier is responsible for the higher extent of mucoadhesive properties.

Films as dosage forms for the buccal route of delivery need to withstand the stress originating from the mechanical activity of the mouth. Adequate mechanical and mucoadhesive characteristics are needed for the films to remain in contact with the mucosa for the desired amount of time of release.[38] Another source of mechanical stress originates from the processes of manufacturing, handling and administration.[39] Thus, to successfully develop films as dosage forms for buccal delivery, a relatively high TS and EB and a low EM are desirable.[38] Additionally, derived from the conventional parameters extracted from stress-versus-strain curves, a relatively high TS/EM, RSE and TI are required.[23,40]

Table 4 shows that adequate control over TS, EB and EM was achieved for FPH01, FPH05 and FPH06; all of which only contained either ERL or ERS and no other polymer. Quaternary ammonium polymethacrylates have been previously described to have suitable properties as film-forming material for dosage forms for the buccal route.[19] In that study we showed that film formulations containing 10% triethylcitrate as plasticizer rendered films with medium TS, high EB and low EM. Here, we have found similar conditions for films that did not contain HPMC as a release modifier polymer. The addition of HPMC was correlated with an increase in TS, decrease in EB and a slight increase in EM (Table 4). This is indicative of less ductile yet more resistant films. The effect of HPMC over the mechanical properties of films is clearer after analysis of the derived mechanical parameters. TS/EM is an indicator of the level of internal stress in a film, the larger its value the higher the film crack resistance. RSE is also used to estimate crack resistance and is approximated from the surface energy of the film. Finally, TI is an estimation of energy absorbed per unit volume of film under stress.[23] FPH01 is the formulation that possessed the largest TS/EM indicating high resistance to cracking (Table 5). The addition of HPMC reduced this value significantly, except for FPH04; however, TS/EM values remained high and acceptable. In the same vein, the

Table 5 Derived mechanical parameters calculated from conventional mechanical properties derived from a stress vs strain plot

Formulation	TS : EM ($\%^{-1}$)	Relative surface energy ($N/mm^2 \cdot \%$)	Toughness index ($N/mm^2 \cdot \%$)
FPH01	5.69 (1.94)[i,ii,iii]	4.59 (1.06)[a]	216.51 (21.32)[i,ii,iii,iv,v]
FPH02	3.36 (0.32)[i]	4.69 (0.63)[a]	92.08 (15.55)[i]
FPH03	3.34 (0.22)[ii]	8.62 (0.77)[b]	88.10 (22.67)[ii]
FPH04	4.11 (0.50)	10.32 (1.93)[b]	60.32 (15.70)[iii,vi]
FPH05	3.88 (0.50)	1.11 (0.08)[c]	89.91 (17.96)[iv]
FPH06	2.77 (0.29)[iii]	1.75 (0.08)[c]	106.33 (20.12)[v,vi]

Results are represented as the mean (SD). EM, elastic modulus; TS, tensile strength. [i–vi]Among parameters, statistically significant differences indicated in pairs of roman numerals ($P < 0.05$). [a–c]Among parameters, non-significant differences are indicated in pairs of letters.

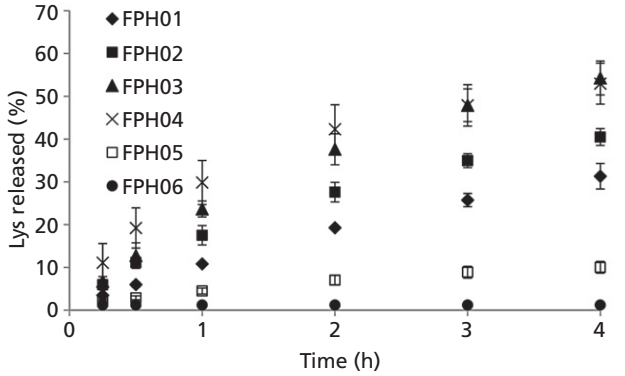

Figure 6 Lys release profiles from particle-containing films FPH01, FPH02, FPH03, FPH04, FPH05 and the control (FPH06) (Data are means ± SD, $n = 6$).

RSE of films increased with increase in the content of HPMC, being highest for FPH04 at 10.32 $N/mm^2 \cdot \%$, indicating crack resistance. Comparison of TI indicates that, except for FPH01 which was shown to be the toughest formulation, the TI of all other formulations varied within an acceptable range (Table 5).

Lysozyme release and kinetics

From the drug release profiles we observed an increase in the release rate and extent of release as the concentration of HPMC increased in the formulations (FPH01–04, Figure 6). HPMC is a water-swellable and water-erodible polymer that will dissolve from the dosage form; therefore, increasing concentrations of HPMC in formulations allow for domains in the film that will release Lys faster than ERL-rich domains. In accordance with the similarity value, f_2,[41] FPH03 and FPH04 were the only formulations that rendered a similar Lys release profile (Table 6). Therefore, an increase in the HPMC content from 30 to 50% w/w of polymer did not elicit significant differences in the release profile. According to the Korsmeyer–Peppas model, even though FPH04 has a higher constant ($k = 0.2800$ for FPH04 and 0.2255 for FPH03) contributing to faster release at earlier times, the higher exponential term of FPH03 ($n = 0.6604$ for FPH03 and 0.4875 for FPH04) allows for faster release at later times. Similar effects have been described before in films combining HPMC and ERL.[42] Among the various materials studied, Hassan *et al.* found that the combination of HPMC and ERL resulted in a lower burst release (< 20% drug released in the first 15 min) and in formulations that only contained HPMC a more rapid release was found to be associated with the swellable soluble matrix that HPMC constitutes in water.[31] Another study conducted by Averineni *et al.* showed the effect of increasing concentrations of HPMC in chitosan-containing film formulations.[43] Over a 210-min period, drug release increased from 52.52 to 73.23% for the formulations containing the lowest and highest amounts of HPMC, respectively.

Table 6 Differences among FPH series of formulations based on the similarity factor, f_2

f2	FPH01	FPH02	FPH03	FPH04	FPH05	FPH06
FPH01	–	40.76	22.47	20.73	27.23	19.40
FPH02		–	34.46	31.64	18.11	12.65
FPH03			–	56.79	9.75	5.89
FPH04				–	9.00	5.29
FPH05					–	45.23
FPH06						–

Release profiles are similar if $f_2 \geq 50$.

In the Kormeyer–Peppas release kinetics model, n is the release exponent, and is an indicator of the drug release mechanism.[44] In the particular case of $n = 0.5$, the drug release mechanism is purely Fickian diffusion (the particular solution that constitutes the Higuchi model equation). When $n = 1$ the equation describes a zero-order release mechanism, and the region in the range of $0.5 < n < 1$ represents the so-called anomalous transport. First-order kinetics applies to dosage forms that normally contain water-soluble drugs and porous polymer matrices. In said systems, drug release is proportional to the amount of drug remaining inside; therefore, the rate of drug release decreases with time. From Table 7 we can observe that, except for FPH04, all formulations exhibit an anomalous

Table 7 Model parameters and adjusted R^2 values for the FPH series of formulations

	Korsmeyer–Peppas $Q = k \times t^{na}$			Higuchi $Q = k \times t^{0.5a}$		First order $Q = k \times (1 - e^{-nt})^a$		
Formulation	k	n	Adj R^2	k	Adj R^2	k	n	Adj R^2
FPH01	0.1092	0.7702	0.9980	0.1407	0.9391	0.4956	0.2474	0.9995
FPH02	0.1728	0.6287	0.9955	0.1943	0.9791	0.4702	0.4672	0.9965
FPH03	0.2255	0.6604	0.9874	0.2612	0.9659	0.6579	0.4335	0.9998
FPH04	0.2800	0.4875	0.9751	0.2769	0.9881	0.5340	0.8316	0.9966
FPH05	0.0457	0.5837	0.9961	0.0492	0.9894	0.1114	0.5380	0.9911

[a]Where Q is the amount of drug released in time t, k is a constant and n is an exponential constant.

release of Lys. This is a consequence of systems that are water-swellable, where drug release occurs by a combination of diffusion and case-II transport. For FPH04, the release is more adequately modelled by the Higuchi model (evidenced by the higher R^2). This indicates that drug release in this system follows Fickian diffusion through the polymer matrix. In addition, all formulations are better adjusted to the first-order kinetics model (according to the R^2). This model describes drug release from porous matrices, such as those formed in a water-swollen polymethacrylate film, containing a water-soluble drug, such as the Lys-containing particles. In this system, drug release is proportional to the amount of drug remaining in the interior of the dosage form.[24] From the release profile we can also observe that when Lys was added to the film formulation as a solid solution very little release was achieved over the 4-h period. Molecules in solid solution are completely surrounded by the polymeric matrix and a higher number of interactions between polymer and Lys can be achieved. This results in a very slow release over the time period (below limit of quantification).

Lysozyme activity remaining after film manufacture

After 24 h of release in dissolution media, the activity of the Lys released was evaluated to measure any decrease in activity, as an indicator of enzyme stability. As depicted in Figure 7, Lys remaining activity was excellent for all the formulations studied revealing that the processing of manufacturing particles into films for buccal delivery did not render the enzyme inactive. As shown above in the characterization of nanoparticles, enzyme activity is not compromised during the manufacturing process, and the results obtained in this section show that further processing into polymeric films does not render the enzyme inactive. FPH05 exhibited a slightly lower activity, which we believe was due to partial release of Lys over the 24-hours period (data not shown).

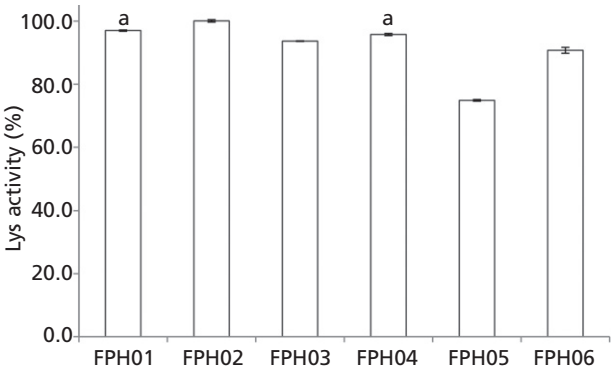

Figure 7 Lys relative activity obtained from infinity release studies from film formulations. a: non-significant difference is indicated in pair of letters.

Conclusions

We have successfully developed PCNP-containing films based on polymer matrices of polymethacrylates and HPMC as delivery vehicles for buccal delivery. Lys-loaded nanoparticles manufactured by our antisolvent precipitation process were incorporated in the films. By controlling the pH and increasing the loading we were able to optimize conditions previously described. The new conditions for the method of manufacture allowed for the production of small and narrowly distributed particles with high loading efficiency and excellent remaining activity. Particles from formulation SPH02 were used in the manufacture of films for buccal delivery. All films containing Lys-coated nanoparticles had acceptable mechanical properties and Eudragit RL was shown to have excellent mucoadhesive properties. Additionally, films were able to sustain the release of Lys over 4 h, modulated to faster release rates by the use of HPMC. Finally, we were able to achieve excellent enzyme activity maintained in films containing Eudragit RL.

Declarations

Conflict of interest

The Author(s) declare(s) that they have no conflicts of interest to disclose.

References

1. Tan ML *et al*. Recent developments in liposomes, microparticles and nanoparticles for protein and peptide drug delivery. *Peptides* 2010; 31: 184–193.
2. Frokjaer S, Otzen DE. Protein drug stability: a formulation challenge. *Nat Rev Drug Discov* 2005; 4: 298–306.
3. Wang W. Instability, stabilization, and formulation of liquid protein pharmaceuticals. *Int J Pharm* 1999; 185: 129–188.
4. Polonsky WH *et al*. Psychological insulin resistance in patients with type 2 diabetes. *Diabetes Care* 2005; 28: 2543–2545.
5. Simmons JH *et al*. Reliability of the diabetes fear of injecting and self-testing questionnaire in pediatric patients with type 1 diabetes. *Diabetes Care* 2007; 30: 987–988.
6. Rubin RR *et al*. Barriers to insulin injection therapy. *Diabetes Educ* 2009; 35: 1014–1022.
7. Müller G. Oral delivery of protein drugs: driver for personalized medicine. *Curr Issues Mol Biol* 2011; 13: 13–24.
8. Singh R *et al*. Past, present, and future technologies for oral delivery of therapeutic proteins. *J Pharm Sci* 2008; 97: 2497–2523.
9. Heinemann L, Jacques Y. Oral insulin and buccal insulin: a critical reappraisal. *J Diabetes Sci Technol* 2009; 3: 568–584.
10. Pather SI *et al*. Current status and the future of buccal drug delivery systems. *Expert Opin Drug Deliv* 2008; 5: 531–542.
11. Salamat-Miller N *et al*. The use of mucoadhesive polymers in buccal drug delivery. *Adv Drug Deliv Rev* 2005; 57: 1666–1691.
12. Morales JO, McConville JT. Manufacture and characterization of mucoadhesive buccal films. *Eur J Pharm Biopharm* 2011; 77: 187–199.
13. Perumal VA *et al*. Investigating a new approach to film casting for enhanced drug content uniformity in polymeric films. *Drug Dev Ind Pharm* 2008; 34: 1036–1047.
14. Ibrahim MA *et al*. Stability of insulin during the erosion of poly(lactic acid) and poly(lactic-co-glycolic acid) microspheres. *J Control Release* 2005; 106: 241–252.
15. Cui F *et al*. Preparation and evaluation of chitosan-ethylenediaminetetraacetic acid hydrogel films for the mucoadhesive transbuccal delivery of insulin. *J Biomed Mater Res A* 2009; 89A: 1063–1071.
16. Giovino C *et al*. Development and characterisation of chitosan films impregnated with insulin loaded PEG-b-PLA nanoparticles (NPs): a potential approach for buccal delivery of macromolecules. *Int J Pharm* 2012; 428: 143–151.
17. Nikolic K *et al*. Self-assembly of nanoparticles on the surface of ionic crystals: structural properties. *Surf Sci* 2007; 601: 2730–2734.
18. Kreiner M *et al*. DNA-coated microcrystals. *Chem Commun* 2005; 21: 2675–2676.
19. Morales JO *et al*. The influence of recrystallized caffeine on water-swellable polymethacrylate mucoadhesive buccal films. *AAPS PharmSciTech* 2013. In press.
20. Morales JO *et al*. A design of experiments to optimize a new manufacturing process for high activity protein-containing submicron particles. *Drug Dev Ind Pharm* 2013. In press.
21. Shugar D. The measurement of lysozyme activity and the ultra-violet inactivation of lysozyme. *Biochim Biophys Acta* 1952; 8: 302–309.
22. Parikh NH *et al*. Tensile properties of free films cast from aqueous ethylcellulose dispersions. *Pharm Res* 1993; 10: 810–815.
23. Okhamafe AO, York P. Stress crack resistance of some pigmented and unpigmented tablet film coating systems. *J Pharm Pharmacol* 1985; 37: 449–454.
24. Costa P, Sousa Lobo JM. Modeling and comparison of dissolution profiles. *Eur J Pharm Biopharm* 2001; 13: 123–133.
25. Tiyaboonchai W *et al*. Formulation and characterization of curcuminoids loaded solid lipid nanoparticles. *Int J Pharm* 2007; 337: 299–306.
26. Schubert MA, Müller-Goymann CC. Characterisation of surface-modified solid lipid nanoparticles (SLN): influence of lecithin and nonionic emulsifier. *Eur J Pharm Biopharm* 2005; 61: 77–86.
27. Kreiner M *et al*. Enzyme-coated micro-crystals: a 1-step method for high activity biocatalyst preparation. *Chem Commun* 2001; 12: 1096–1097.
28. Jores K *et al*. Investigations on the structure of solid lipid nanoparticles (SLN) and oil-loaded solid lipid nanoparticles by photon correlation spectroscopy, field-flow fractionation and transmission electron microscopy. *J Control Release* 2004; 95: 217–227.
29. Mora-Huertas CE *et al*. Polymer-based nanocapsules for drug delivery. *Int J Pharm* 2010; 385: 113–142.
30. Murdan S *et al*. Immobilisation of vaccines onto micro-crystals for enhanced thermal stability. *Int J Pharm* 2005; 296: 117–121.
31. Colombo P. Swelling-controlled release in hydrogel matrices for oral route. *Adv Drug Deliv Rev* 1993; 11: 37–57.
32. Ham AS *et al*. Vaginal film drug delivery of the pyrimidinedione IQP-0528 for the prevention of HIV infection. *Pharm Res* 2012; 29: 1897–1907.
33. Smart JD. The role of water movement and polymer hydration in mucoadhesion. In: Mathiowitz E et al., ed. *Bioadhesive Drug Delivery Systems: Fundamentals, Novel Approaches, and Development*. New York: Marcel Dekker Inc, 1999: 11–23.
34. Panomsuk SP *et al*. A study of the hydrophilic cellulose matrix: effect of drugs on swelling properties. *Chem Pharm Bull* 1996; 44: 1039–1042.
35. Nafee NA *et al*. Mucoadhesive buccal patches of miconazole nitrate: in vitro/in vivo performance and effect of ageing. *Int J Pharm* 2003; 264: 1–14.
36. Asane GS *et al*. Polymers for mucoadhesive drug delivery system: a current status. *Drug Dev Ind Pharm* 2008; 34: 1246–1266.

37. Wong CF *et al.* Formulation and evaluation of controlled release Eudragit buccal patches. *Int J Pharm* 1999; 178: 11–22.
38. Peh KK, Wong CF. Polymeric films as vehicle for buccal delivery: swelling, mechanical, and bioadhesive properties. *J Pharm Pharm Sci.* 1999; 2: 53–61.
39. Perumal VA *et al.* Formulation of monolayered films with drug and polymers of opposing solubilities. *Int J Pharm* 2008; 358: 184–191.
40. Omari DM *et al.* Lactic acid-induced modifications in films of Eudragit RL and RS aqueous dispersions. *Int J Pharm* 2004; 274: 85–96.
41. Moore JW, Flanner HH. Mathematical comparison of dissolution profiles. *Pharm Tech* 1996; 20: 64–74.
42. Hassan MA *et al.* Formulation and in vitro/in vivo evaluation of naproxen mucoadhesive buccal patches for local effect. *J Drug Deliv Sci Technol* 2011; 21: 423–431.
43. Averineni RK *et al.* Development of mucoadhesive buccal films for the treatment of oral sub-mucous fibrosis: a preliminary study. *Pharm Dev Technol* 2009; 14: 199–207.
44. Korsmeyer RW *et al.* Mechanisms of solute release from porous hydrophilic polymers. *Int J Pharm* 1983; 15: 25–35.